JBAT 12(1) (2023) 78 – 86

Jurnal Bahan Alam Terbarukan

Accredited SINTA 2 by Ministry of Research and Technology/National Research and Innovation Agency
SK No. 200/M/KPT/2020
http://journal.unnes.ac.id/nju/index.php/jbat

p-ISSN 2303 0623
e-ISSN 2407 2370

Synthesis and Characterization of Metal-Organic Framework as Battery Electrodes

Sutikno Madnasri[1,✉], Teguh Darsono[1], Isa Akhlis[1], Heru Saputera[1], Meilody Indreswari[1], Lutfiana Maghfirotul Izza[1], Maria A Simangunsong[1], Lambang Setyo Utama[2], Uda Hashim[3]

DOI: https://doi.org/10.15294/jbat.v12i1.44170

[1] Physics Department, Faculty of Mathematics and Natural Sciences, Universitas Negeri Semarang Sekaran Campus, Gunungpati, Semarang, Indonesia, 50229
[2] Electrical Engineering Department, Faculty of Engineering, Universitas Negeri Semarang, Sekaran Campus, Gunungpati, Semarang, Indonesia, 50229
[3] Institute of Nano Electronic Engineering (INEE), University Malaysia Perlis, 02600, Arau, Perlis, Malaysia

Article Info

Article history:
Received
1 April 2023
Revised
15 May 2023
Accepted
3 June 2023
Online
20 June 2023

Keywords:
Electrode;
Metal-organic framework;
Organic battery;
Synthesis;
Sodium-ion

Abstract

Metal organic framework-derived carbons (MOFDCs) are materials with great potential and can be used as electrochemical energy storage because these have a large surface area and pore structure that can be adapted to needs. MOFs have porous crystals in which metal ions or clusters are linked by organic ligands. The purpose of this study was to determine the physical and electrochemical properties of MOF5 synthesized at different temperatures. The MOFs synthesis method which is classified as complicated can be simplified and the use of hazardous solvents can be reduced by means of partial substitution using water solvents. To prepare MOFs can be done in several ways, such as liquid phase epitaxy, supersonic cold spraying, direct gas phase preparation, and interface-assisted synthesis. MOFs have applications in optics, sensing, catalysis, adsorption, and modeling, as well as electrochemical energy storage. Potential application as an interesting electrode material to be studied through the synthesis method. In this study, MOF5 was synthesized at temperatures between 200°C-600°C. To prepare MOF5, zinc nitrate tetrahydrate and acetic acid were dissolved in DMF (N, N-dimethyl formamide). The remaining precipitate (MOF) was immersed three times in DMF and three times in chloroform for 24 hours for each immersion. In general, different MOF5 synthesis affects the microstructure, elemental content, optical properties (transmittance and absorbance), electrical properties, and electrochemical properties.

INTRODUCTION

A metal-organic framework (MOF) is a porous solid formed by coordination bonds between organic ligands and metal ions or clusters (Xie et al., 2020; Bennett & Cheetham, 2014). MOFs are conductive to electric charges and have many potential applications such as gas adsorption (Chen et al., 2019), electrocatalysis, sensor, energy storage material (Xie et al., 2020), gas separation or storage, membrane, magnetic remembrance (Zheng et al., 2021), three-dimensional patterning, non-linear optics, and white lighting source (Cui et al., 2016). MOFs are mainly used as self-sacrificing templates or porous carbon sources (Zhou et al., 2020). Metal-organic frameworks (MOFs) have been reported to improve the performance of Si-based anode materials due to their three-dimensional (3D) framework and organic/inorganic ligands.

In recent years, various MOFs with large internal spaces and open channels for ion pathways through crystal structures have been of great interest to researchers as alternatives for energy storage and conversion (Boutaybi et al., 2020; Choi et al., 2021). MOFs have diverse and manageable chemical compositions and structures, and many catalytic sites (Zhang et al., 2021; Barthel et al., 2018). Through high-temperature pyrolysis or controlled

✉ Corresponding author:
E-mail: smadnasri@yahoo.com

chemical reactions, MOFs can be easily synthesized into metal compounds with a porous three-dimensional composition and crystal structure (An et al., 2021) and adjustable pore size and shape (Zhang et al., 2021), because the MOF has compatibility with aqueous solutions, and long cycle life (1000 cycles). Generally, the sodium ion battery anode material obtained by using MOF as a precursor displays a rich pore structure, which is conducive to fully exposing the active site and thereby improving the electrochemical reaction kinetics of the battery system (Choi et al., 2021). In addition, MOF-derived heteroatom-rich carbon can generate external defects to further enhance the conductivity of the carbon matrix (Li et al., 2021).

Problems encountered in the charging/discharging capability of metal-air batteries are still limited by the slow reaction kinetics of oxygen reduction reactions or oxygen evolution reactions (Yang et al., 2016; Kumar et al., 2021). Materials such as inorganic metal oxides and silicon are also used as electrodes but have the disadvantage of slow diffusion of metal oxide ions, which causes a slow charging or discharging rate of the battery. Likewise, the presence of variations in the electrode volume induces mechanical instability (Boutaybi et al., 2020). The amount of charge storage is also influenced by the morphology of the active ingredient (Zhang et al., 2021). This research was aimed to determine the physical and electrochemical properties of MOF5 at different synthesis temperatures. By optimizing the synthesis temperature, it is hoped that MOF5 with superior physical and electrochemical properties can be obtained.

MATERIALS AND METHODS

The materials used in this study consisted of zinc nitrate tetrahydrate (Sigma Aldrich), DMF (N, N-dimethyl formamide) (Sigma Aldrich), acetic acid, chloroform, 2-methyl imidazolate (Sigma Aldrich), and methanol. The equipment used includes measuring cups, balances, crucibles, magnetic stirrers, and furnaces.

To prepare MOF5, 1 g of zinc nitrate tetrahydrate and 0.1 g of acetic acid were dissolved in 40 ml of DMF. The solution was stirred using a magnetic stirrer for about 20 minutes and transferred to a crucible without a lid to be heated using a furnace (Thermo Fisher Scientific, Thermolyne FB1410M-33) at temperatures of 200°C-600°C for 4 hours. The remaining precipitate (MOF) was immersed three times in DMF and three times in chloroform for 24 hours for each immersion. Then, the MOF was drained and burned without a lid in a furnace at 150°C for 2 hours.

The microstructures of MOF5 were observed using a scanning electron microscope (Thermo Fisher Scientific, Phenom Pro X) and their crystal structures were determined using an X-ray diffractometer (Malvern Panalytical, Netherlands). To determine the optical properties of MOF5, Fourier Transform Infra-Red (FTIR PerkinElmer, L182105) and UV-vis spectrophotometer (Shimadzu, UV-2600i) were used.

RESULTS AND DISCUSSION

MOFs are novel crystalline porous materials with outstanding structure, compositional and morphological features and have been widely used in energy storage and conversion fields. Various pure MOFs and their derivatives have been developed and used as anode materials in lithium-ion batteries (Reddy et al., 2020). MOF is used as anode material in the manufacture of organic batteries. The synthesis method developed in this research is slow evaporation or solvothermal (Chuhadiya et al., 2021) which is a direct synthesis method. Heating was carried out without a lid for 8 hours and heating with a lid for 2 hours. The surface microstructures of the MOFs made at (a) 200 °C, (b) 300 °C, (c) 400 °C, (d) 500 °C, and (e) 600 °C are shown in Figure 1. They seem that the increase in heating temperature from 200 °C to 600 °C during the synthesis causes the particles to get smaller, the particle density is higher, and the porosity is lower. The particles have a spherical shape (Yan et al., 2021). The smaller the pores, the smaller the more active sites for lithium ions. Therefore, MOF5 synthesized at low heating temperatures (200 °C – 300 °C), many active sites for lithium ions are found (Yan et al., 2021). In general, MOFs have a high surface area and porosity properties (Chuhadiya et al., 2021). MOF5 has high microporosity with significant concentrations of 5 and 10 wide pores (Ingersoll et al., 2019).

Energy Dispersive X-ray Spectroscopy curve to determine the composition of the synthesized MOF at (a) 200 °C, (b) 300 °C, (c) 400 °C, (d) 500 °C, and (e) 600 °C such as shown in

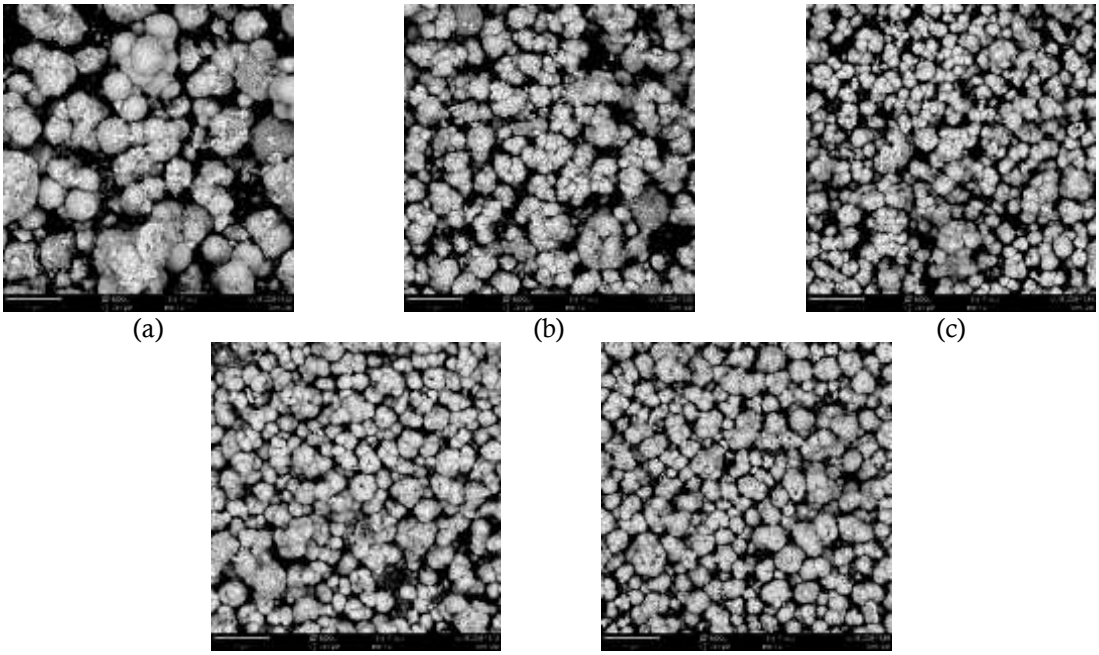

Figure 1. Microstructure of synthesized MOF at temperatures of (a) 200 °C (b) 300 °C (c) 400 °C (d) 500 °C (e) 600 °C.

Figure 2. The detected elements appear on the EDS curve, namely Zn, O, C, and N with high-intensity peaks (Zhou et al., 2020). Nitrogen content is quite small coincides with carbon. The element Zn (Zinc) appears to have a dominant peak, followed by a carbon peak. Quantitatively, the levels of elements in the resulting MOF are shown in Table 1. The increase in heating temperature from 200 °C to 600 °C causes the zinc content of the resulting MOF to tend to increase from 56.99%w to 72.13%w. Meanwhile, the level of oxygen in the resulting MOF tends to decrease from 29.26 %w to 22.33 %w. The levels of carbon and nitrogen elements also tend to decrease.

The levels of elements in the composition of the synthesized MOF at ((a) 200 °C, (b) 300 °C, (c) 400 °C, (d) 500 °C, and (e) 600 °C are shown in Table 1. Based on table 1, the higher the heating temperature, the higher the zinc content, while the lower the oxygen content.

The crystal structures of the MOFs are formed from metal ions and organic binders and are characterized using an X-ray diffractometer (XRD) (Chuhadiya et al., 2021). The XRD curves of the synthesized MOF at (a) 200 °C, (b) 300 °C, (c) 400 °C, (d) 500 °C, and (e) 600 °C as shown in Figure 3. There can be seen that heating from 200 °C to 600 °C does not change the crystal structure of the MOF. This is consistent with the results of research published by (Jeong et al., 2017). Three peaks of high intensities were found at two theta angles of 31.75°, 34.42°, and 36.24°. This is a short-range order (Bennett & Cheetham, 2014). In the short-range regular chain structure Zn, C, N, and O elements were found. This structure is in line with the crystal structure pattern published by previous researchers (Zhou et al., 2021). The next three peaks are found at two theta angles of 47.55°, 56.55°, and 62.85°. This is a long-range order structure (Bennett & Cheetham, 2014). Based on the comparison of MOF1 and MOF5 (Denisov et al., 2019; Shi et al., 2021), it is certainly that MOF5 was successfully produced in this study as shown according to the diffraction pattern in Figure 3. The resulted MOF of direct synthesis is in the form of crystalline thin films (Chuhadiya et al., 2021). For MOF1, three high-intensity peaks were found at two theta angles of less than 15°. Likewise, for the MOF2 diffraction pattern, three high-intensity peaks were found at two theta angles of less than 15° (Getachew et al., 2014). MOF5 has a cubic crystal structure (Zeng et al., 2021).

The results of the optical properties characterization of MOF materials in the form of transmittance data (%) to wavelength (cm^{-1}). This data was obtained from the MOF sample test using FTIR. FTIR curves of synthesized MOF samples at (a) 200 °C, (b) 300 °C, (c) 400 °C, (d) 500 °C, and (e) 600 °C as shown in Figure 4. An increased heating temperature causes an increase in the

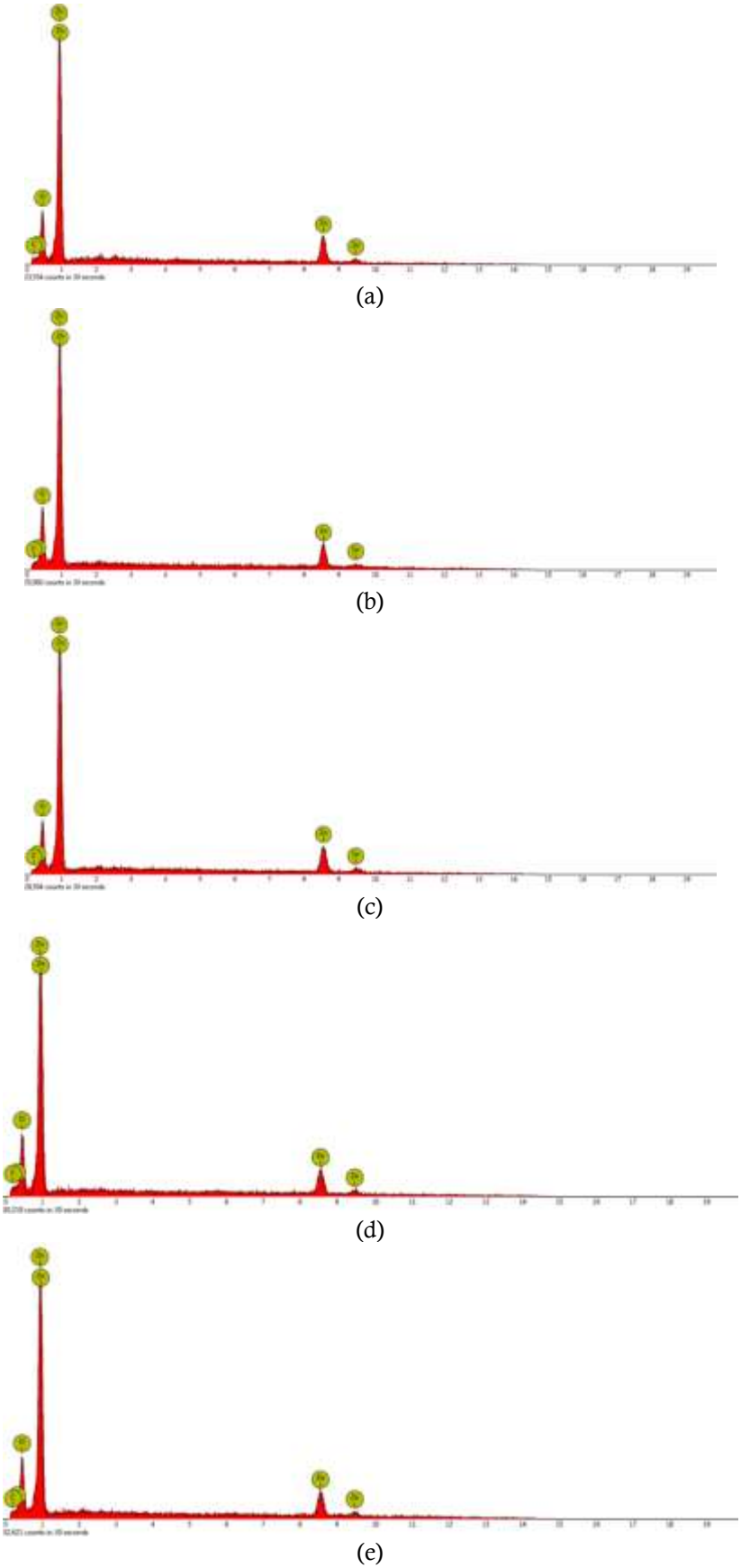

(a)

(b)

(c)

(d)

(e)

Figure 2. The synthesized EDS MOF curves at temperatures of (a) 200 °C, (b) 300 °C, (c) 400 °C, (d) 500 °C, and (e) 600 °C.

Table 1. Composition of synthesized MOF at temperatures (a) 200 °C, (b) 300 °C, (c) 400 °C, (d) 500 °C, and (e) 600 °C.

Element	Weight Percentages (%w)				
	200 °C	300 °C	400 °C	500 °C	600 °C
Zn	56.99	59.65	64.85	63.79	72.13
O	29.26	29.99	26.46	25.80	22.33
N	7.38	4.32	5.10	4.55	4.16
C	6.38	6.04	3.58	5.86	1.38

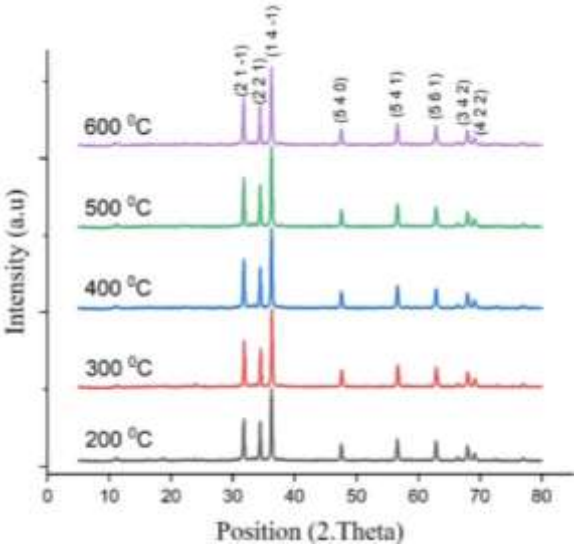

Figure 3. Diffraction pattern of synthesized MOF in the temperature range of 200 °C – 600 °C.

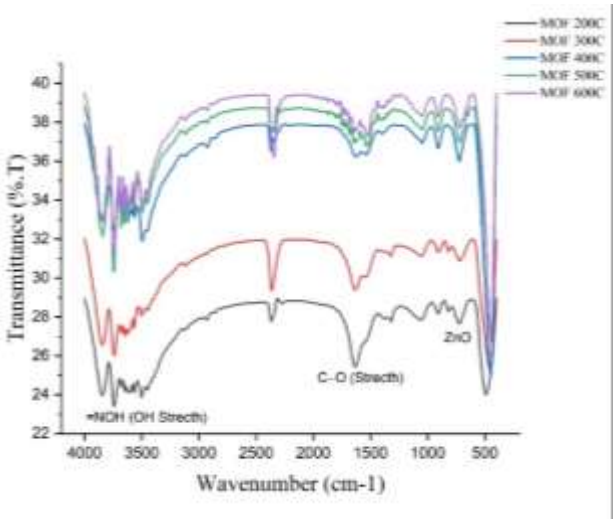

Figure 4. FTIR curves of the synthesized MOF in the temperature range of 200 °C – 600 °C.

resulting MOF transmittance. MOF synthesized at 600 °C has the highest transmittance or lowest absorbance. What is interesting is that there is the sharpest increase in transmittance from a heating temperature of 300 °C to a heating temperature of 400 °C, because it appears to be the largest. Materials that have high transmittance mean low absorbance values. The highest absorbance peak was found in the synthesized MOF at a temperature of 200 °C (Shi et al., 2021; Getachew et al., 2014; Zeng et al., 2021). The peaks that appear at wavenumbers around 3409 cm^{-1}, 2827 cm^{-1}, 2503 cm^{-1}, 1380 cm^{-1}, and 1550 cm^{-1} are -OH, -CH, -COOH, and C=C, respectively (Cheng et al., 2021; Ensafi et al., 2021; Fang et al., 2021).

The highest absorbance was found in samples whose synthesis process was through heating at 500 °C. It was found that in the heating temperature range of 200 °C – 500 °C, the higher the heating temperature caused the MOF absorbance to increase. However, the MOF heating results at a temperature of 600 °C showed the smallest absorbance (Wang et al., 2020a; Chen et al., 2021). The highest absorbance, 2.25, was found in the synthesized sample at a temperature of 500 °C, and the lowest absorbance, 1.75, was found in the sample heated to 200 °C. In the ultraviolet wavelength region (200 nm – 350 nm), the MOF has good absorbance, while in the visible light wavelength, 350 nm – 600 nm, the absorbance decreases until it approaches 0.5. As shown in Figure 5, MOF's ability to absorb visible light is decreasing. Functional groups containing oxygen can cause a catalytic effect. The non-polar bonding of carbon materials is not conducive to adsorption and cannot prevent the shuttle effect well (Chen et al., 2021).

The electrical properties of the MOF were studied using an Elkahfi I-V meter. The results of current versus voltage measurements for synthesized MOF materials at (a) 200 °C, (b) 300 °C, (c) 400 °C, (d) 500 °C, and (e) 600 °C as shown in Figure 6. The synthesized MOF with a heating temperature of 200 °C appears to be the most

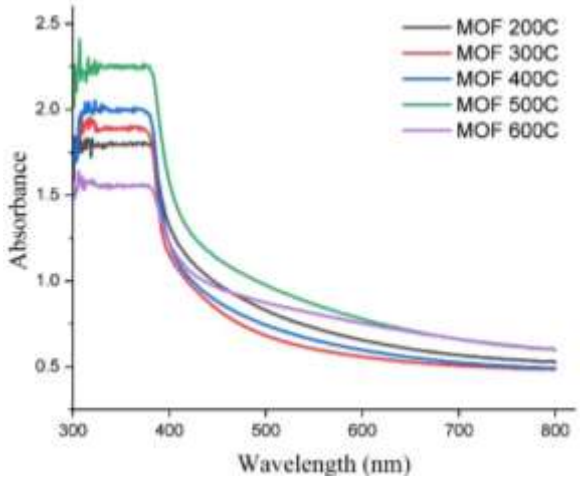

Figure 5. Spectra UV vis MOF synthesized at temperatures of 200 °C – 600 °C.

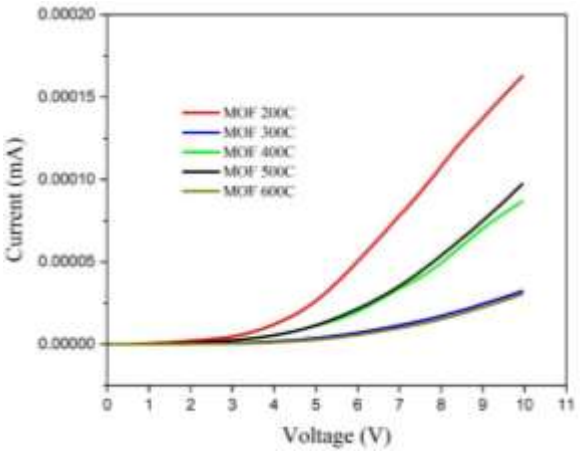

Figure 6. Currents versus voltage curves of the synthesized MOF at temperatures of 200 °C – 600 °C.

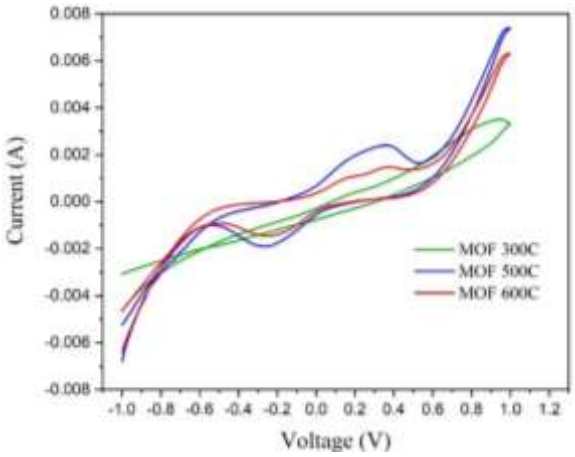

Figure 7. Cyclic voltammetry graph of MOF5.

conductive, the generated current is the highest (Wang et al. 2020b; Muthurasu et al., 2021). At a voltage of 10 V, the electric current generated from the samples through the heating process of 200 °C, 300 °C, 400 °C, 500 °C, and 600 °C respectively is $1.77.10^{-4}$ mA, $2.58.10^{-5}$ mA, $7.17.10^{-5}$ mA, $9.74.10^{-5}$ mA, and $3.02.10^{-5}$ mA. From Figure 1, the synthesis process at the lowest temperature, 200 °C, resulted in the MOF sample with the largest porosity. These more pores serve as a place to accommodate oxygen so that the oxygen evolution reaction activity is superior (Wang et al., 2020b; Tan et al., 2021). The increase in temperature from 300 °C to 500 °C produces MOF which can generate an increasing electric current as well. According to EDX data, Zn levels increased, while C levels decreased. At high temperatures, the C bonds are broken, and the ZnO compound increases. ZnO is the main contributor to the increase in MOF conductivity, because the electrical conductivity of ZnO is quite high, around 10^4 $\Omega^{-1}cm^{-1}$. Meanwhile, the synthesized MOF at 200 °C showed the highest current, while the synthesized MOF at 600 °C showed the lowest current.

Figure 7 shows the cyclic voltammetry graph of the synthesized MOF thin film at temperatures of 300 °C, 500 °C, and 600 °C. The generated cyclic current is the scan result at a voltage of -1 V to 1 V. The higher the MOF heating temperature, the generated current appears at a smaller initial and final voltage. When the potential is increased from -0.65 V to 1 V, two valleys appear at -0.5 V and 0.5 V, while when the scan is continued in the opposite direction, from 1 V to -0.65 V, a peak appears at 0.35 V. This peak indicates that a cathodic oxygen reduction reaction has occurred (Muthurasu et al., 2021; Tan et al., 2021; Shang et al., 2021). The shape of the voltammetric curve that is formed shows the sign of a Faradaik type battery (Wang et al., 2021). Different MOF

synthesis temperatures have different effects on the generated currents. The tendency, higher synthesis temperature, results in a more conductive MOF, the generated current tends to increase. The higher the temperature, the higher the peak current generated is greater. A porous and uniform material has a shorter diffusion trail length, facilitating electrons and electrolyte ions to reach the redox center quickly (Wang et al., 2021).

CONCLUSION

It can be concluded that the higher the synthesis temperature, the smaller the MOF5 microporosity size and the higher the MOF5 grain density. The increase in heating temperature in the synthesis of MOF5 causes zinc levels to increase, while oxygen, nitrogen, and carbon levels decrease. XRD MOF5 results produced at a synthesis temperature between 200°C-600°C shows the same three strong peaks, namely in the angle range 2θ between 30° and 40°. Based on FTIR data, the transmittance of the synthesized MOF5 in the temperature range of 200°C-600°C worth between 20%-40%, and the higher the synthesis temperature, the higher the transmittance. The absorbance value of MOF5 has not shown consistent results with increasing the synthesis temperature. At the same voltage, the synthesized MOF5 at a lower temperature indicates a higher electric current generated. The electrochemical properties of MOF5 showed that at the synthesis temperature of 500 °C, a dominant peak appeared compared to the synthesized MOF5 at temperatures of 300 °C and 600 °C.

ACKNOWLEDGEMENTS

We express our gratitude to the Research and Community Service Institute, Universitas Negeri Semarang, through the Fundamental Research Grant Scheme under the Rectors's Decree on Research and Community Service Number B/317/UN37/HK/2023.

REFERENCES

An, Y., Tan, S., Liu, Y., Zhu, K., Hu, L., Rong, Y., An, Q. 2021 Designs and applications of multi-functional covalent organic frameworks in rechargeable batteries. Energy Storage Materials. 41: 354–379.

Barthel, S., Alexandrov, E. V., Proserpio, D. M., Smit, B. 2018. Distinguishing metal-organic frameworks. crystal growth & design. 18: 1738−1747.

Bennett, T. D., Cheetham, A. K. 2014. Amorphous Metal−Organic Frameworks. Accounts of Chemical Research. 47 (5): 1555−1562.

Boutaybi, M. E., Taleb, A., Touzani, R., Bahari, Z. 2020. Metal-organic frameworks based on pyrazole subunit for batteries applications: A systematic review. Materials Today Proceeding. 31: S96–S102.

Chen, P., Ren, H., Yan, L., Shen, J., Wang, T., Li, G., Chen, S., Cong, X., Xie, J., Li, W. 2019. Metal−organic frameworks enabled high-performance separators for safety-reinforced lithium-ion battery. ACS Sustainable Chemical Engineering. 7: 16612−16619.

Cui, Y., Li, B., He, H., Zhou, W., Chen, B., Qian, G. 2016. Metal−organic frameworks as platforms for functional materials. Accounts of Chemical Research. 49: 483−493.

Choi, D., Lim, S., Han, D. 2021. Advanced metal-organic frameworks for aqueous sodium-ion rechargeable batteries. Journal of Energy Chemistry. 53: 396–406.

Chuhadiya, S., Himanshu, Suthar, D. Patel, S. L., Dhaka, M. S. 2021. Metal-organic frameworks as hybrid porous materials for energy storage and conversion devices: A review. Coordination Chemistry Reviews 446: 214115.

Chen, J., Feng, W., Zhao, W., Shi, Z. 2021. Transition metal phosphide composite with metal-organic framework and carbon nanotubes for high-performance lithium-sulfur batteries. Journal of Alloys and Compounds. 890 (2021): 161794.

Cheng, L., Chen, J., Yan, Y., Zhang, J., Hu, H., Zhang, J., Luo, Y., Chen, Y. Wang, G.,Wang, R. 2021. Metal-organic frameworks derived active functional groups decorated manganese monoxide for aqueous zinc ion battery. Chemical Physics Letters. 778: 138772.

Denisov, G. L., Primakov, P. V., Korlyukov, A. A., Novikov, V. V., Nelyubina, Y. V. 2019. Solvothermal Synthesis of the Metal-Organic Framework MOF-5 in Autoclaves Prepared by 3D Printing. Russian Journal

of Coordination Chemistry. 45(12): 836–842.

Ensafi, A. A., Heydari-Soureshjani, E., Taghipour-Jahromi, A. R., Rezaei, B. 2021. Bimetallic metal organic framework-derived for both battery-like supercapacitor (electrolyte study) and hydrogen evolution reaction. Electrochimica Acta. 395: 139192.

Fang, Y., Chen, Y., Zeng, L., Yang, T., Xu, Q., Wang, Y., Zeng, S., Qian, Q., Wei, M., Qinghua, C. 2021. Nitrogen-doped carbon encapsulated zinc vanadate polyhedron engineered from a metal-organic framework as a stable anode for alkali ion batteries. Journal of Colloid and Interface Science. 593: 251–265.

Getachew, N., Chebude Y., Diaz, I., Sanchez-Sanchez, M. 2014. Room temperature synthesis of metal-organic framework MOF-2. Journal of Porous Materials. 21(5): 769–773.

Ingersoll, N., Karimi, Z., Patel, D., Underwood, R., Warren, R. 2019. Metal-organic framework-derived carbon structures for sodium-ion battery anodes. Electrochimica Acta. 297: 129-136.

Jeong, S., Kim, D., Park, J., Shin, S., Kim, H., Jeong, G. H., Moon, D., Moon, H. R., Lah, M. S. 2017. Topology conversions of non-interpenetrated metal−organic frameworks to doubly interpenetrated metal−organic frameworks. Chemistry of Materials. 29(9): 3899−3907.

Kumar, P., Goyal, S. K., Singh, B. P. 2021. Application of bifunctional catalysts and metal-organic frameworks in metal-air batteries for renewable power conversion applications Materials Today Proceeding. 43: 2839–2842.

Li, X., Xiang, Y., Deng, R., Wei, X., Liu, X., Zheng, Q., Lin, D., Song, Y. 2021. Metal-organic frameworks-derived multi-shell copper-cobalt-zinc sulfide cubes for sodium-ion battery anode. Chemical Engineering Science. 425: 131501.

Muthurasu, A., Tiwari, A. P., Chhetri, K., Dahal, B., Kim, H. Y. 2021. Construction of iron-doped cobalt- vanadate- cobalt oxide with metal-organic framework oriented nanoflakes for portable rechargeable zinc-air batteries powered total water splitting. Nano Energy. 88: 106238.

Reddy, R. C. K., Lin, J., Chen, Y., Zeng, C., Lin, X., Cai, Y., Su, C. Y. 2020. Progress of nanostructured metal oxides derived from metal-organic frameworks as anode materials for lithium-ion batteries. Coordination Chemistry Reviews. 420: 213434.

Shi, X., Shan, Y., Du, M., Pang, H. 2021. Synthesis and application of metal-organic framework films. Coordination Chemistry Reviews. 444: 214060.

Shang, H., Jin, D., Hu, L. K. K., Wang, X., Ding, Y., Lin, H., Rui, K., Zhu, J., Huang, W. 2021. Metal-organic framework-derived carbon decorated Ni–Sn nanostructures for ultrastable metal-ion batteries Composites Communications. 25: 100724.

Tan, H., Zhou, Y., Qiao, S. Z., Fan, H. J. 2021. Metal-organic framework (MOF) in aqueous energy devices. Materials Today. 48: 270-284.

Wang, K., Bi, R., Huang, M., Lv, B., Wang, H., Li, C., Wu, H., Zhang, Q. 2020a. Porous cobalt metal−organic frameworks as active elements in battery−supercapacitor hybrid devices. Inorganic Chemistry. 59: 6808-6814.

Wang, X., Ge, L., Lu, Q., Dai, J., Guan, D., Ran, R., Weng, S. C., Hu, Z., Zhou, W., Shao, Z. 2020b. High-performance metal-organic framework-perovskite hybrid as an important component of the air-electrode for rechargeable Zn-Air battery. Journal of Power Sources. 468: 228377.

Wang, S., Huang, F., Zhang, Z., Cai, W., Jie, Y., Wang, S., Yan, P., Jiao, S., Cao, R. 2021. Conductive metal-organic frameworks promoting polysulfides transformation in lithium-sulfur batteries. Journal of Energy Chemistry.

Xie, L. S., Skorupskii, G., Dinca, M. 2020. Electrically conductive metal−organic frameworks. Chemistry Reviews. 120: 8536-8580.

Yang, J., Ma, Z., Gao, W., Wei, M. 2016. Layered structural Co-based MOF with conductive network frames as a new supercapacitor electrode. Chemistry – A European Journal. 23(3): 631 – 636.

Yan, Z., Liu, J., Lin, Y., Deng, Z., He, X., Ren, J., He, P., Pang, C., Xiao, C., Yang, D., Yu, H., Du, N. 2021. Metal-organic frameworks-derived CoMOF-D@Si@C core-shell structure for high-performance lithium-ion battery anode, Electrochimica Acta. 390: 138814.

Zheng, S., Wang, Q., Hou, Y., Li, L., Tao, Z. 2021. Recent progress and strategies toward high-performance zinc-organic batteries. Journal of Energy Chemistry.

Zhou, J., Yu, X., Zhou, J., Lu, B. 2020. Polyimide/metal-organic framework hybrid for high-performance Al - Organic battery. Energy Storage Materials. 31: 58–63.

Zhang, X., Li, G., Zhang, Y., Luo, D., Yu, A., Wang, X., Chen, Z. 2021. Amorphizing metal-organic framework towards multifunctional polysulfide barrier for high-performance lithium-sulfur batteries. Nano Energy. 86: 106094.

Zhou, J., Zhang, G., Luo, J., Hu, Y., Hao, G., Guo, H., Guo, F., Wang, S.,Jiang, W. 2021. A MOFs-derived 3D superstructure nanocomposite as excellent microwave absorber. Chemical Engineering Science. 426: 130725.

Zeng, S., Ye, L., Guo, Y., Gao, Q., Wu, Q., Xu, W. 2021. Cubic metal-organic framework as an electro-catalytic for Li-S batteries. Materials Letter. 297: 129942.